2022 International Symposium on Nonlinear Theory and Its Applications,
NOLTA2022, Virtual, December 12-15, 2022

Nonlinear Trends Extraction for COVID-19 Daily New Cases in Japan

Fumihiko Ishiyama

NTT Space Environment and Energy Labs., Nippon Telegraph and Telephone Corp.
3-9-11, Midori-cho, Musasino, Tokyo, 180-8585, Japan
Email: fumihiko.ishiyama@ntt.com

Abstract—We have developed a nonlinear method of time series analysis, that allows us to obtain multiple nonlinear trends from a given set of numerical data. We propose to apply the method to recognize the ongoing status of COVID-19 infection, and applied to the time series of daily new cases in Japan. We found that there is only a single nonlinear trend, and this result justifies the use of a week-based infection growth rate as an index. In addition, the fitting with the obtained nonlinear trend holds for a duration of more than three months for the Delta variant infection time series. The fitting also visualizes the transition to the Omicron variant.

1. Introduction

Understanding the COVID-19 infection status, such as "what's going on?" and "what happens next?", has been a major issue in the last couple of years.

Various forecasting methods have been studied to address this issue. Among them, machine learning (ML) based studies have played a major role. For example, various methods such as Linear Regression (LR), Least Absolute Shrinkage and Selection Operator (LASSO), Support Vector Machine (SVM), and Exponential Smoothing (ES) were compared to achieve better prediction [1]. In addition, other methods such as Auto-Regressive Integrated Moving Average (ARIMA) based approach [2], and Gaussian Process Regression (GPR) based approach [3] were also studied for forecasting.

In contrast to their focusing on "what happens next?", we focus on "what's happening now?" in this paper. That is, we propose a framework to recognize nonlinear phenomena, and apply the framework to COVID-19 infection time series to recognize "what happens now".

We have a unique nonlinear method of time series analysis that provides an analytical perspective on numerically obtained nonlinear time series [4, 5, 6], and we apply the method to COVID-19 daily new cases in Japan.

As there are no similar conventional methods, we show an example of obtained results with our method in a previous work [7] to illustrate our approach.

Figure 1(a) shows a numerically calculated time series $S(t)$ of a gravitational wave named A1B3G3 which corresponds to black hole generation at $t = t_0$ [8]. We applied our method to the time series before the black hole generation $t < t_0$.

Time series $S(t)$ with multiple nonlinear trends $\lambda_m(t)$ is expressed in the form of $S(t) = \sum_m \exp\int \lambda_m(t)dt$, and the fitted $\lambda_m(t)$ with our method are plotted in Fig. 1(b).

It should be noted that a linear system $dx/dt - \lambda x = 0$ has constant $\lambda(t) = \lambda$, and its corresponding time series becomes $\exp\int \lambda(t)dt = \exp\lambda t$. That is, non-constant $\lambda(t)$ means that the analyzed system is nonlinear. Note also that a linear system with multiple λ_m is written as $\left[\prod_m (d/dt - \lambda_m)\right] x = 0$.

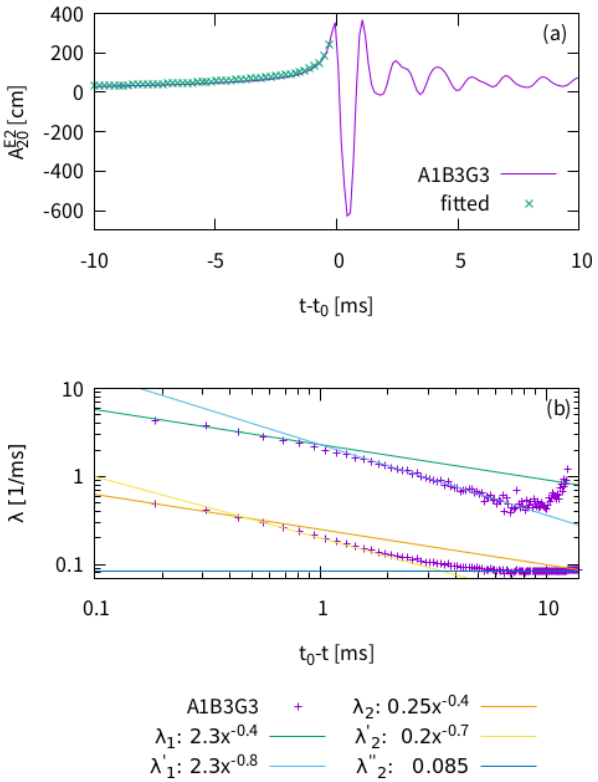

Figure 1: Example of nonlinear analysis. (a) Time series for analysis, and (b) obtained nonlinear trends.

Obtained nonlinear trends just before $t = t_0$ are

$$\lambda_1(t) = 2.3(t_0 - t)^{-0.4} \quad (1)$$

$$\lambda_2(t) = 0.25(t_0 - t)^{-0.4}, \quad (2)$$

ORCID iDs Fumihiko Ishiyama: 0000-0002-1375-494X

and the corresponding time series becomes

$$\begin{aligned} S_0(t) &\simeq 702e^{\int_{t_0}^{t}\lambda_1(\tau)d\tau} + 168e^{\int_{t_0}^{t}\lambda_2(\tau)d\tau} \\ &= 702e^{2.3\int_{t_0}^{t}(t_0-\tau)^{-0.4}d\tau} + 168e^{0.25\int_{t_0}^{t}(t_0-\tau)^{-0.4}d\tau} \\ &= 702e^{-\frac{2.3}{0.6}(t_0-t)^{0.6}} + 168e^{-\frac{0.25}{0.6}(t_0-t)^{0.6}}. \end{aligned} \quad (3)$$

The fitted time series Eq. (3) is plotted in Fig. 1(a). The time series around $t_0 - t \sim 2$ ms and $t_0 - t > 10$ ms are

$$S_1(t) \simeq 29e^{-\frac{2.3}{0.2}(t_0-t)^{0.2}} + 96e^{-\frac{0.2}{0.3}(t_0-t)^{0.3}} \quad (4)$$

$$S_2(t) \simeq 29e^{-0.085(t_0-t)} \quad (5)$$

respectively. Each equation corresponds to each phase.

This kind of analytical expression becomes possible with our method, and we apply the method to a COVID-19 infection time series.

In the following sections, we introduce our method of analysis, apply the method to the analysis of a COVID-19 time series, and finally, we conclude the paper.

2. Method

Our method is based on a mode decomposition with general complex functions, which organize nonlinear oscillators [4, 5, 6], and we calculate the local linearized solution of the decomposition.

Nonlinear trends extraction is a part of our method. Obtained nonlinear oscillators with zero frequency correspond to nonlinear trends.

2.1. Model Equation

We expand the given time series $S(t) \in \mathbb{R}$ with general complex functions $H_m(t) \in \mathbb{C}$ as

$$S(t) = \sum_{m=1}^{M} e^{H_m(t)}, \quad (6)$$

where M is the number of the complex functions.

The complex functions are expressed as

$$H_m(t) = \ln c_m(t_0) + \int_{t_0}^{t} [2\pi i f_m(\tau) + \lambda_m(\tau)]\mathrm{d}\tau, \quad (7)$$

where $f_m(t) \in \mathbb{R}$ represents the frequency modulation (FM) terms [9], which are known as instantaneous frequencies, $\lambda_m(t) \in \mathbb{R}$ represents the amplitude modulation (AM) terms, which correspond to our original [4, 5, 6] nonlinear trends, and $c_m(t_0) \in \mathbb{C}$ represents the amplitudes of the oscillators at $t = t_0$.

This expansion corresponds to a mode decomposition with general complex functions, noting that

$$H'_m(t) = 2\pi i f_m(t) + \lambda_m(t). \quad (8)$$

2.2. Local Linearized Solution

As it is known that our model equation Eq. (6) does not have a unique solution, due to the nonlinearity [10], we need an additional concept to make our model equation uniquely solvable. For this purpose, we apply a local linearization technique

$$S(t)|_{t\sim t_k} \simeq \sum_{m=1}^{M} e^{H_m(t_k)+H'_m(t_k)(t-t_k)+O((t-t_k)^2)} \quad (9)$$

around $t \sim t_k = t_0 + k\Delta T$, consider a short enough time width, and ignore the higher order terms $O((t-t_k)^2)$ [11].

Then, the equation becomes a simple linear equation

$$S(t)|_{t\sim t_k} \simeq \sum_{m=1}^{M} e^{H_m(t_k)+H'_m(t_k)(t-t_k)}, \quad (10)$$

and we can obtain unique $H'_m(t_k)$ easily by using the linear predictive coding (LPC) method with N samples, noting that we must use a non-standard numerical method to solve LPC [6, 12].

Next, we calculate the complex amplitudes $c_m(t_k)$ of the oscillators $c_m(t_k)e^{H'_m(t_k)(t-t_k)}$ as

$$\arg\min_{c_m(t_k)} \sum_{n=0}^{N-1} \left(S(t_k + n\Delta T) - \sum_{m=1}^{M} c_m(t_k) e^{nH'_m(t_k)\Delta T} \right)^2, \quad (11)$$

and we obtain a local linearized solution

$$S(t)|_{t\sim t_k} \simeq \sum_{m=1}^{M} c_m(t_k) e^{[2\pi i f_m(t_k)+\lambda_m(t_k)](t-t_k)}. \quad (12)$$

2.3. Related Methods

We list major conventional methods in Table 1 [6].

Table 1: Comparison with major conventional methods.

	FM	AM	Comment
Our method	$f_m(t)$	$\lambda_m(t)$	calc. both funcs.
AR models	f_m	$\lambda_m < 0$	time-invariant
DFT	$m/M\Delta T$	0	prefixed freqs.
STFT	$m/M\Delta T$	0	time-variant c_m

FM terms $f_m(t)$ and AM terms $\lambda_m(t)$ for the conventional methods are time-invariant, meaning that they are linear methods.

Auto-Regressive (AR) models, such as LPC and Maximum Entropy Method (MEM), use a Tœplitz matrix as an autocorrelation matrix, and time-invariant $\lambda_m(t) = \lambda_m$ is limited to negative values [12]. In addition, they do not calculate complex amplitudes c_m. Prony's method [13] is a kind of AR model, which calculates c_m. However, Prony's method is a historical one (published in 1795), and the method is considered only for reference.

Fourier transform methods such as the Discrete Fourier transform (DFT) and Short-Time Fourier Transform

(STFT) do not calculate $f_m(t)$, and they use prefixed time-invariant frequencies $f_m(t) = m/M\Delta T$. They calculate c_m of corresponding prefixed frequencies. In addition, they ignore $\lambda_m(t)$, because they focus on periodic cases.

3. Analysis

We used the WHO's COVID-19 global data [14] for analysis, and selected the time series of daily new cases in Japan.

Parameters for the analysis were set to $M = 7$, $N = 14$. That is, we used two weeks width data for single analysis, and we plot the results in weekly basis as shown in Fig. 2. Note that major results are not affected by the parameters, in contrast to conventional methods [12].

We show the time series for analysis $S(t)$ in Fig. 2(a), obtained nonlinear trends $\lambda_m(t)$ in Fig. 2(b), and $|c_m(t)|$ vs $f_m(t)$, which corresponds to the spectrum, in Fig. 2(c).

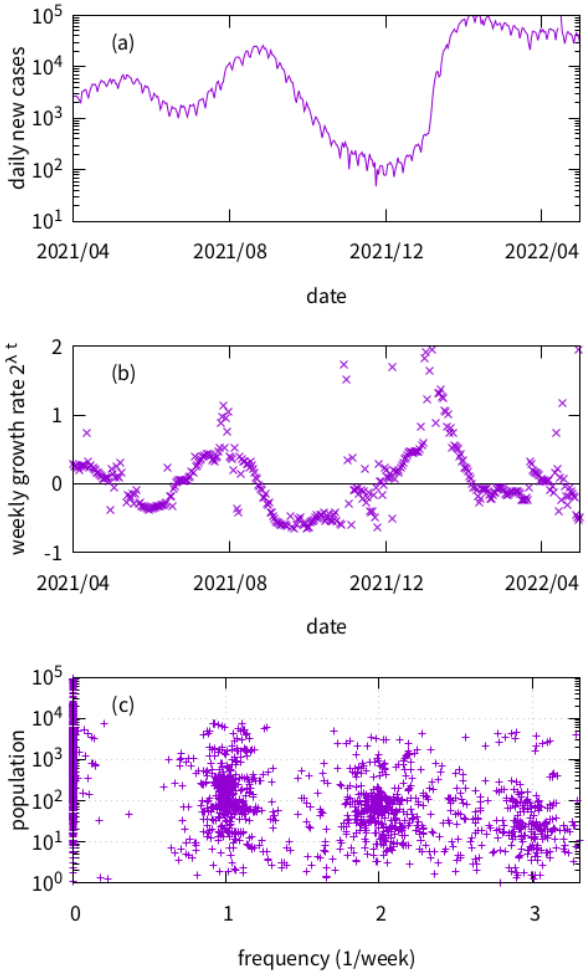

Figure 2: Daily new cases in Japan. (a) Time series for analysis, (b) obtained nonlinear trends, and (c) spectrum.

In contrast to the previous case shown in Fig. 1, multiple nonlinear trends are not evident in Fig. 2(b). The system seems to have a single nonlinear trend, which holds for other countries also. The reason for this will be explained in a further study.

The plotted time seres in Fig. 2(b) correspond to the plots at the zero frequency region $f = 0$ in Fig. 2(c). Weekly oscillation $f = 1$, and its second and third harmonics are also plotted in Fig. 2(c). As we focus on the nonlinear trends, these harmonics are not preferable terms.

As the system seems to have a single nonlinear trend, simplified analysis becomes possible. That is,

$$\lambda(t) = \log_2 \frac{\sum_{\tau=t-6}^{t} S(\tau)}{\sum_{\tau=t-13}^{t-7} S(\tau)}, \tag{13}$$

where weekly summation is used to suppress weekly periodicity and its higher harmonics shown in Fig. 2(c). This equation is known as the week-based infection growth rate, and is justified only when there is a single nonlinear trend.

We apply Eq. (13) to the Delta to Omicron variant transition in Japan, and show in Fig. 3.

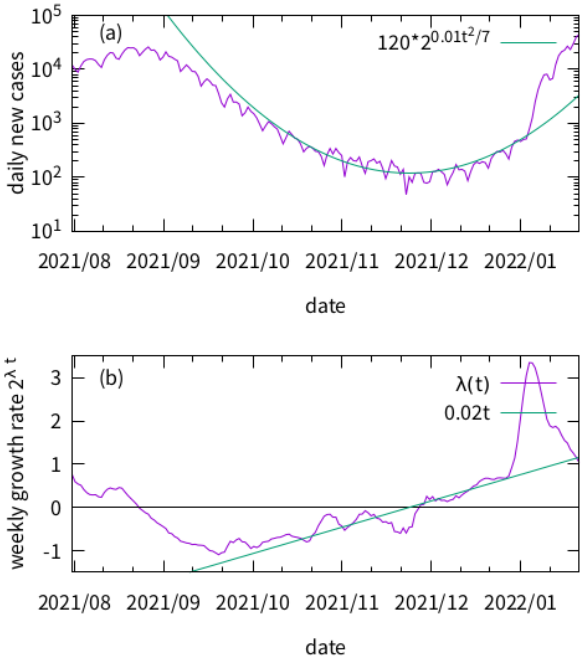

Figure 3: Delta to Omicron variant transition. (a) Time series for analysis, and (b) obtained nonlinear trend.

Fitted line in Fig. 3(b) is the week-based nonlinear trend of the Delta variant

$$\lambda(t) = 0.02(t - t_0), \tag{14}$$

where t_0 is 24/Nov/2021, and corresponding time series

$$S(t) = 120 \cdot 2^{0.01(t-t_0)^2/7} \tag{15}$$

is plotted in Fig. 3(a). This fitted line holds from Sept/2021 to Jan/2022, meaning that the infection status maintained

the nonlinear trend for over three months, and the transition to the Omicron variant happened in Jan/2022. The Delta variant was replaced by the Omicron variant at that time, and the extrapolated line in Fig. 3(b) after the replacement will no longer hold. Another fitting for the Omicron variant is required.

Obtained nonlinear time series Eq. (15) is explained as follows. A time series $s(t)$ with a parameter p and with a lowest order perturbation term ϵt becomes

$$s(t) \propto e^{\int_0^t p+\epsilon\tau d\tau} = e^{pt+\frac{1}{2}\epsilon t^2} = ce^{\frac{1}{2}\epsilon(t-t_0)^2}, \qquad (16)$$

where t_0 is the time of zero crossing, and c is the corresponding amplitude. The linear term p disappears, and the nonlinear term ϵ takes the place.

4. Conclusion

We demonstrated a nonlinear analysis that provides an analytical perspective on a given numerical time series. We focused on the extraction of nonlinear trends $\lambda_m(t) \propto t^{\alpha_m}$, where α_m corresponds to the index of nonlinearity, noting that $\alpha_m = 0$ is the linear case.

We applied our method to a time series of COVID-19 daily new cases in Japan, and found that there is only a single nonlinear trend. This result justifies the use of a week-based growth rate index.

The obtained nonlinear trend was $\lambda(t) \propto t$, and the fitting holds for the Delta variant infection status for a duration exceeding three months. The fitting also visualized the transition to the Omicron variant.

The obtained nonlinear trend $\lambda(t) \propto t$ was also observed in another work [15], and this characteristics will be found widely, because of the universality of Eq. (16).

References

[1] F. Rustam et al., "COVID-19 future forecasting using supervised machine learning models," *IEEE Access,* vol. 8, pp. 101489-101499, 2020.
DOI: 10.1109/ACCESS.2020.2997311.

[2] S. Vanahalli and P. N, "An intelligent system to forecast COVID-19 pandemic using hybrid neural network," in *Proc. 10th IEEE Int. Conf. Commun. Syst. Netw. Tech. (CSNT),* pp. 543-548, 2021.
DOI: 10.1109/CSNT51715.2021.9509622

[3] Y. Alali, F. Harrou and Y. Sun, "Optimized Gaussian process regression by Bayesian optimization to forecast COVID-19 spread in India and Brazil: a comparative study," in *Proc. Int. Conf. ICT Smart Soc. (ICISS),* pp. 1-6, 2021.
DOI: 10.1109/ICISS53185.2021.9532501

[4] F. Ishiyama, "Local linear predictive coding for high resolution time-frequency analysis," in *Proc. 17th IEEE Int. Symp. Signal Process. Info. Tech. (ISSPIT),* pp. 1-6, 2017.
DOI: 10.1109/ISSPIT.2017.8388309

[5] F. Ishiyama, "Piecewise linear predictive coding for nonlinear signal analysis and automatic trend extraction," *IEICE Trans. Fundamentals (Japanese Edition)*, vol. J101-A, pp. 36-45, 2018.

[6] F. Ishiyama, "Constructing nonlinear signal processing theory for characterization and identification of electromagnetic noise sources, and its feasibility study," Ph. D. Thesis, *Tsukuba Univ.*, 2021.
DOI: 10.15068/0002000757

[7] F. Ishiyama, and R. Takahashi, "The bounce hardness index of gravitational waves," *Class. Quant. Grav.,* vol. 27, 245021 (11pp), arXiv:1009.0608, 2010.
DOI: 10.1088/0264-9381/27/24/245021

[8] H. Dimmelmeier, J. A. Font and E. Müller, "Relativistic simulations of rotational core collapse II. Collapse dynamics and gravitational radiation," *Astron. Astrophys.,* vol. 393, pp. 523-542, 2002.
DOI: 10.1051/0004-6361:20021053

[9] B. van der Pol, "The fundamental principles of frequency modulation," *J. Inst. Elect. Eng. III,* vol. 93, pp. 153-158, 1946.

[10] I. Daubechies, J. Lu and H. T. Wu, "Synchrosqueezed wavelet transforms: An empirical mode decomposition-like tool," *Appl. Comput. Harmon. Anal.*, vol. 30, pp. 243-261, 2011.

[11] R. Kubo, "Statistical-mechanical theory of irreversible process. I. General theory and simple applications to magnetic and conduction problems," *J. Phys. Soc. Jpn.,* vol. 12, pp. 570-586, 1957.

[12] F. Ishiyama, "Maximum entropy method without false peaks with exact numerical equation," *J. Phys.: Conf. Ser.,* vol. 1438, 012031 (6pp), 2020.
DOI: 10.1088/1742-6596/1438/1/012031

[13] R. Prony, "Essai expérimental et analytique - Sur les lois de la Dilatabilité des fluides élastiques et sur celles de la Force expansive de la vapeur de l'eau et de la vapeur de l'alkool, à différentes températures," *J. l'École Polytechnique*, vol. 1, Floréal et Plairial III, pp. 24-76, 1795.

[14] https://covid19.who.int/WHO-COVID-19-global-data.csv

[15] F. Ishiyama and M. Maruyama, "Nonlinear time-frequency analysis of lightning strike surge current waveforms recorded at Gasing hill, Kuala Lumpur," in *Proc. 18th IEEE Int. Colloq. Signal Process. Appl. (CSPA),* pp. 20-23, 2022.
DOI: 10.1109/CSPA55076.2022.9782060